The forgotten denominator, pillar loading

K.A. Heasley
National Institute of Occupational Safety and Health, Pittsburg, Pa., USA

ABSTRACT: In the last few decades, a considerable amount of effort was directed at accurately determining the coal/pillar strength to use for safely designing coal mines. The outcome of this early work was the well known Obert-Duvall, Holland-Gaddy, Bieniawski, and Salamon-Munro equations for coal pillar strength. All of these equations were developed for, and were calibrated with, pillars in a large room-and-pillar area such that the loading could be determined using the "tributary-area" theory. In order to account for the abutment loads associated with full-extraction mining, the empirical methods have typically adopted a simple conceptualization of the abutment load through use of an "abutment angle." Short of a complete numerical or analytical analysis of the coal seam and surrounding strata, very little work has been directed toward refining the empirical analysis of pillar loading. It appears that the vast majority of the research has been directed at determining the pillar strength, the numerator of the safety factor equation, when the denominator of the safety factor equation, the pillar loading, plays an equally important role in pillar design. This paper will address the deficit of pillar loading research by exploring the accuracy of the empirical abutment load calculations using insight provided by an elastic overburden model, a laminated overburden model and field observations. Ultimately, it is determined that a constant abutment angle probably over-predicts the abutment load as the mining depth increases.

INTRODUCTION

In the last few decades, a considerable amount of effort has been directed at accurately determining the coal pillar strength to use for safely designing coal mines. Some of the first scientific research in this area consisted of determining the relationship between coal strength and the shape and size of laboratory and field specimens (Gaddy 1956, Holland 1964, Obert & Duvall 1967, Bieniawski 1968, Wagner 1974, Hustrulid 1976). These experimentally-derived relationships between coal strength, and specimen shape and size were then used to develop formulas for estimating pillar strength in the field. A further refinement of this empirical technique for determining pillar strength was to use a statistical analysis of pillar performance in the field in order to enhance the parameters of the experimentally-determined size and shape equation or to provide a factor of safety for practical application of the equation (Holland 1964, Salamon & Munro 1967, Bieniawski 1983). The outcome of this early work was the well-known Obert-Duvall, Holland-Gaddy, Bieniawski, and Salamon-Munro equations for coal pillar strength. These empirical equations have been validated through many years of actual use and encapsulate considerable knowledge of coal pillar behavior into a simple practical form (Mark & Iannacchione 1992). All of these equations were developed for, and were calibrated with, pillars in a large room-and-pillar area such that the loading could be determined using the "tributary-area" theory.

As longwall mining became more prevalent, the classic pillar design equations (Mark & Iannacchione 1992) were extended to designing pillars for gateroads. In order to account for the abutment loads associated with full-extraction mining, the empirical methods have typically

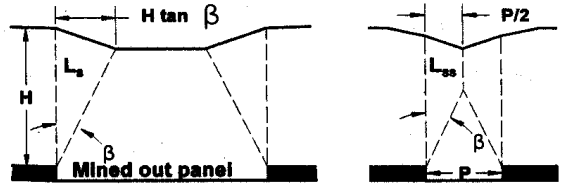

Figure 1. The conceptualization of a side abutment load angle (after Mark, 1992).

adopted a simple conceptualization of the abutment load through the use of an "abutment angle". In this concept, the abutment load is the weight of the wedge of overburden material defined by the abutment angle (β) and a vertical line at the edge of the panel (see Figure 1, after Mark 1992). Also, in response to the gateroad pillar design problem, a new and more complex concept of pillar behavior based on a confined core surrounded by a crushed or yielded coal zone was developed and advocated (Wilson 1973, Barron & Pen 1992, Salamon 1992). In the original confined core design method, the abutment loads were calculated using the abutment angle technique. More recently, the complete deformation of the rock mass-coal system has been analyzed for determining the pillar behavior and loading conditions (Salamon 1992, Hasenfus & Su 1992, Park 1992).

Short of a complete numerical or analytical analysis of the coal seam and surrounding strata, very little work has been directed toward refining the empirical abutment angle analysis of pillar loading. It appears that the vast majority of the research has been directed at determining the pillar strength, the numerator of the safety factor equation, when the denominator of the safety factor equation, the pillar loading, plays an equally important role in pillar design. Recently, some field measurements in Australia (Colwell et al. 1999) and observations in the United States (Mark & Chase 1997) have indicated that the constant abutment angle concept for pillar loading may need some refinement. This paper will address the deficit of pillar loading research by exploring the accuracy of the empirical abutment load calculations using insight provided by an elastic overburden model, a laminated overburden model and field observations.

ABUTMENT LOADING - DISTRIBUTION

It is informative to investigate abutment loading and the differences in abutment loading calculations used by various empirical pillar design and analytical modeling techniques. First, let's examine the empirical Analysis of Longwall Pillar Stability (ALPS) method (Mark 1990) which is widely used to help design pillars in longwall gateroads. For the ALPS method, Mark (1990) tabulated numerous field measurements of abutment loads where he found that the measured distribution of induced abutment stress (σ_f) follows the equation:

$$\sigma_f(x) = \frac{3 L_s}{(D_s - L)^3}(D_s - x)^2 \qquad (1)$$

where: x = the distance from the center of the panel,
L = the half width of the panel,
L_s = the total side abutment load,
D_s = the maximum horizontal extent of the abutment stress from the panel edge.
($x > L$ and $x < D_s$)

The maximum horizontal extent of the abutment stress was also determined from field measurements (Peng & Chiang 1984, Mark 1990) to be equal to (in metric units):

$$D_s = L + 9.3\sqrt{0.3048\,H} \qquad (2)$$

where: H = the depth of overburden (see Figure 2, after Mark 1992).

(Equations 1 and 2 were modified from Mark's original formula by shifting the x origin from the edge of the panel to the center of the panel to be consistent with the following derivations for the homogeneous and laminated overburden models. Also, the units were converted to metric units.)

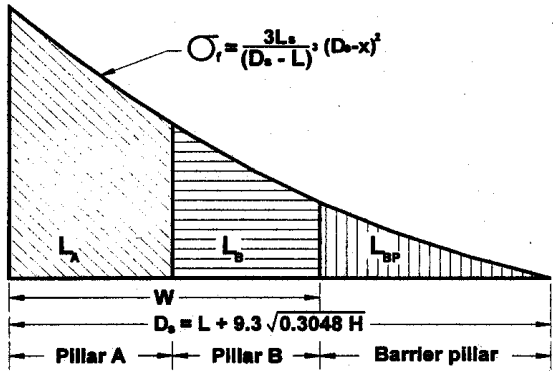

Figure 2. Distribution of the side abutment load (after Mark, 1992).

Next, consider the analytical abutment stress predicted at the edge of a two-dimensional slot in an infinite, homogeneous, isotropic, elastic model (σ_h) as given by (Salamon 1964):

$$\sigma_h(x) = \frac{x\,q}{\sqrt{x^2 - L^2}} \qquad (for\ x > L) \qquad (3)$$

where the virgin in situ stress (q) can be written as:

$$q = \gamma H \qquad (4)$$

with: γ = the overburden density.

This equation provides the stress distribution at the edge of a theoretical longwall panel where: (1) the coal seam and overburden are all one elastic material, (2) the width of the panel is negligible in comparison to the depth, and (3) the thickness of the seam is negligible in comparison to the width of the panel. It is interesting to note that equation 3 is independent of material properties, and because of the assumptions in the derivation, the seam thickness does not appear in the equation.

Finally, consider the analytical abutment stress predicted at the edge of a two-dimensional slot in the laminated overburden model (σ_l) with "homogeneous stratifications" as represented by LAMODEL (Heasley 1998).

$$\sigma_l(x) = qL\sqrt{\frac{2E_s}{E\lambda M}}\, e^{-\sqrt{\frac{2E_s}{E\lambda M}}(x-L)} \qquad (5)$$

where: E_s = the elastic modulus of the seam,
E = the elastic modulus of the overburden,
M = the extraction thickness,
(for $x > L$)
and the lamination constant, λ, is defined as:

$$\lambda = \sqrt{\frac{t^2}{12(1-\nu^2)}} \qquad (6)$$

where: t = the lamination thickness,
ν = the Poisson's Ratio of the overburden.

In order to plot and compare the abutment stresses computed from equations 1, 3 and 5, some "typical" values were assumed for the geometric and rock mass parameters: a panel width of 200 m (L = 100 m), an overburden depth (H) of 160 m (q = 4 MPa), an extraction thickness (M) of 2 m, an elastic modulus of the rock mass (E) of 20 GPa, a Poisson's Ratio (ν) of the rock mass of 0.25, a lamination thickness (t) of 15 m, and no gob load (L_s = qL). Using these values for the parameters, the abutment stresses at the edge of a simulated panel for the empirical ALPS formula (equation 1), the homogeneous elastic overburden formula (equation 3), and the laminated overburden formula (equation 5) are plotted in Figure 3. (It should be noted that equations 1 and 5 calculate induced stresses, and that equation 3 calculates the total stress. Therefore, in the plots, the virgin overburden stress (q) has been added to the results from equations 1 and 5 to provide a direct comparison with the total abutment stress values from equation 3.)

In Figure 3, it can be seen that the homogeneous elastic abutment stress has a relatively sharp, infinite

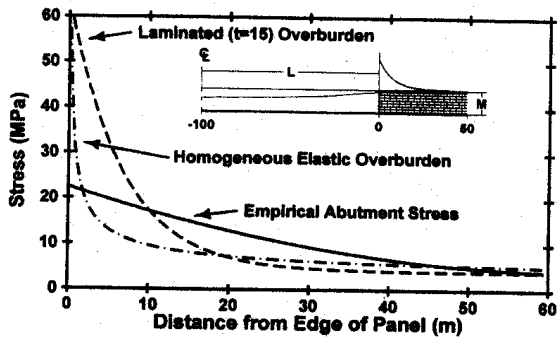

Figure 3. Comparison of the longwall abutment stress computed from the homogeneous elastic model, the laminated model and the empirical formula.

peak at the edge of the panel and approaches virgin vertical stress asymptotically with increasing distance from the panel. In contrast, the abutment stress in the laminated overburden is finite at the panel edge and asymptotically approaches the virgin overburden stress (q) less rapidly. Neither of these

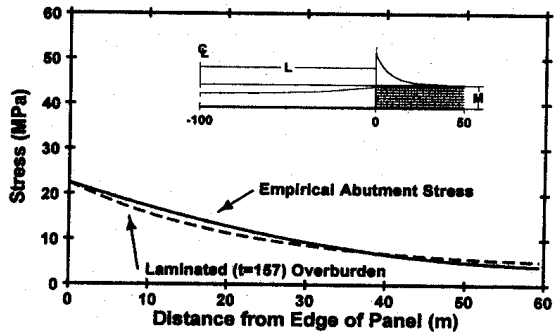

Figure 4. Plot of the laminated abutment stress fitted to the empirical formula.

mathematical models (using the assumed parameters) comes very close to matching the empirical abutment stress curve which is much flatter.

However, if the abutment stress level in the laminated model and the stress level obtained from the empirical formula are equated at the edge of the seam (x=L):

$$\sigma_l(L) = qL\sqrt{\frac{2E_s}{E\lambda M}} = \frac{3L_s}{D_s - L} = \sigma_f(L) \qquad (7)$$

Then, by expanding λ, L_s, and D_s, and solving for the lamination thickness (t), the value of t which ensures this equality can be determined as:

$$t = 20.29\sqrt{1-\nu^2}\,\frac{E_s H}{E M} \qquad (8)$$

For a typical seam modulus (E_s) of 2 GPa in the laminated model, equation 8 provides a fitted lamination thickness of 157 m. The plot of the abutment stress curve for the laminated overburden model with a fitted lamination thickness of 157 m is shown together with the empirically determined abutment stress in Figure 4. The degree of agreement between the two curves is very good, but the lamination thickness of 157 m needed to provide this degree of fit is unrealistic.

Additional insight about abutment loading can be gained by taking a even closer look at the abutment load distribution (the shape of the curves) as represented by the empirical formula (equation 1) and the laminated model (equation 5). First, assume that the total overburden load is carried on the abutments (there is no gob load), then:

$$L_s = qL = \gamma HL \qquad (9)$$

and if equation 1 is expanded using equation 2 andonly the stress at the edge of the panel is considered, the peak abutment load is:

$$\sigma_f(L) = (0.5843)\,\gamma\sqrt{H}L \qquad (10)$$

This equation shows that the empirically-determined peak abutment stress at the edge of the panel is directly proportional to the overburden density (γ) and the panel half-width (L). These relationships seem intuitively logical. Equation 10 also shows that the magnitude of the empirical abutment stress is proportional to the square root of the depth. This is an interesting result. However, if one considers equation 2 which shows that the extent of the empirical abutment stress is also proportional to the square root of the depth, then the combination of these two relationships would give the logical result that the total abutment load is directly proportional to the depth.

If equation 5 for the laminated overburden model is similarly expanded using equation 6, and only the stress at the edge of the panel is considered, then the following relationship results:

$$\sigma_l(L) = (2.632)\,\gamma HL\sqrt{\frac{E_s\sqrt{1-\nu^2}}{EMt}} \qquad (11)$$

In equation 11, the peak abutment stress at the edge of the panel for the laminated model is also directly proportional to the overburden density (γ) and the panel half-width (L) as was the peak abutment stress for the empirical formula. However, equation 11 shows that the peak stress for the laminated model is directly proportional to the depth (H) as opposed to being proportional to the square root of the depth, as was the case for the empirical formula. Equation 11 also shows that the peak abutment stress for the laminated model is directly proportional to the square root of the seam modulus (E_s) and inversely proportional to the square root of the overburden modulus (E), extraction thickness (M) and lamination thickness (t). These last relationships all seem reasonable considering that elastic plate theory was used to derive the laminated model. However, if these relationships are reasonable, why are the relationships not sufficiently evident in the empirical data to have been incorporated into equation 1?

The effect of depth needs to be more closely examined. In previous work, it was determined that for optimum subsidence prediction with the laminated model, the lamination thickness should increase with depth (Yang 1992, Salamon 1989).

To formalize this relationship, Yang proposed an inherent overburden constant, ω.

$$\omega = \sqrt{\frac{H\sqrt{3\,(1-\nu^2)}}{t}} \qquad (12)$$

In later work with subsidence prediction using the laminated model, the same trend toward increasing lamination thickness with increasing depth was also found (Heasley & Barton 1998). Similarly, when modeling stresses with the laminated model, it was found that the optimum lamination thickness is proportional to the area-of-interest, such that thinner laminations were best for modeling the small scale inter-seam pillar stresses, but thicker laminations were optimum for modeling wide area longwall abutment stresses (Heasley 1998).

If the value of ω is indeed a constant for the given strata, then equation 12 implies that the lamination thickness should be directly proportional to the depth (rearranging equation 12):

$$t = \frac{H\sqrt{3\,(1-\nu^2)}}{\omega^2} \qquad (13)$$

If equation 13 is then substituted back into equation 11:

$$\sigma_l(L) = 2\,\gamma\sqrt{H}L\,\omega\sqrt{\frac{E_s}{EM}} \qquad (14)$$

This equation now shows that the peak abutment stress for the laminated model is proportional to the square root of the depth (H), similar to the peak abutment stress for the empirical ALPS formula as shown in equation 10.

Equation 14 still indicates that the peak abutment stress for the laminated model is directly proportional to the square root of the seam modulus (E_s) and inversely proportional to the square root of the overburden modulus (E) and the extraction thickness (M). For most coal measure rocks, the ratio of the seam modulus to the overall overburden modulus will probably remain fairly constant between different mines and not greatly affect the relative value of the peak abutment stress. Conversely, the extraction thickness (M) distinctly varies between different mines and it is shown to be inversely proportional to the peak abutment stress for the laminated model. This means that thicker seams will have lower peak abutment stresses and tend to spread the abutment load over a larger distance from the panel. This result (derived from the laminated model) suggests that the seam thickness is an important factor to consider in determining the distribution of the abutment stress at the edge of an extraction panel.

ABUTMENT LOADING - MAGNITUDE

In addition to the load distribution, the other factor to determine regarding the abutment load is the magnitude. In ALPS, a simple geometric conceptualization utilizing an abutment angle (β) is used (see Figure 1). The magnitude of the side abutment load (L_s) is calculated as the weight of the overburden within a wedge defined by this abutment angle and a vertical line from the edge of the panel. For a supercritical panel the formula is:

$$L_s = H^2 (\tan \beta) (\gamma/2) \qquad (15)$$

and for a subcritical panel the formula is:

$$L_{ss} = \left[\left(\frac{HP}{2} \right) - \left(\frac{P^2}{8 \tan \beta} \right) \right] \gamma \qquad (16)$$

where: P = the panel width

A panel is subcritical when:

$$\frac{H}{P} > \frac{1}{2 (\tan \beta)} \qquad (17)$$

With the recommended value of $\beta = 21°$ (Mark 1992), the transition from supercritical to subcritical occurs at a depth-to-width ratio (H/P) of about 1.3.

In order to investigate the change in the magnitude of abutment loading with depth, the equations for the side abutment load can be normalized by dividing through by half the total load (L_t) over the longwall panel in order to calculate a percentage load

$$L_t = \frac{\gamma H P}{2} \qquad (18)$$

Then, the side abutment load equations can be further normalized by writing them as a function of the ratio of panel depth to panel width (H/P). For the supercritical case (equation 15), the result is:

$$\frac{L_s}{L_t} = \frac{H}{P} (\tan \beta) \qquad (19)$$

For the subcritical case (equation 16), the normalization result is:

$$\frac{L_{ss}}{L_t} = \left| 1 - \left(\frac{1}{\left(\frac{H}{P} \right) 4 (\tan \beta)} \right) \right| \qquad (20)$$

These last two equations show that the percentage of the total panel cover load that results in the side abutment load is linear with relation to the depth-to-width ratio up to the transition point from supercritical to subcritical. After the transition, the percentage of side abutment load for subcritical

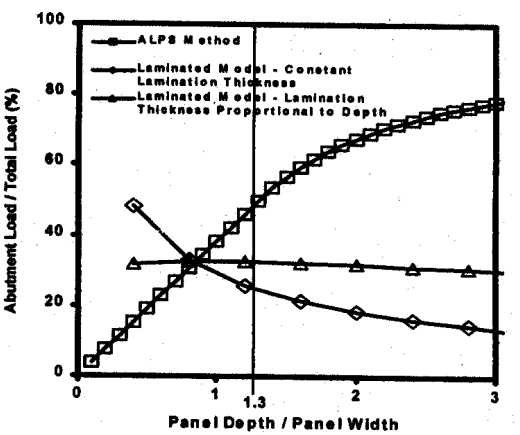

Figure 5. A comparison of the percentage magnitude of the abutment load between the ALPS method and the laminated overburden model.

panels asymptotically approaches 100% as the depth-to-width ratio increases. The relationship between the percentage of total panel load that goes into the side abutment load and the panel depth-to-width ratio is shown in Figure 5. The ALPS method essentially implies that, for a given panel width, the gob load is constant for a seam deeper than a depth-to-width ratio (H/P) of about 1.3. Therefore, the gob load in a 200 m wide panel at a depth of 240 m would be identical to the gob load in a 200 m wide panel at a depth of 600 m. This relationship does not seem intuitively reasonable and conflicts with the behavior implied by the homogeneous-elastic and the laminated models as will be shown below.

With the homogeneous elastic or the laminated overburden model, the magnitude of the abutment load is determined by a complex interaction between the displacement of the overburden, and the compaction and support provided by the gob material. However, some intuition into the depth-related response of the abutment load can be gained by closely examining the analytical displacement functions for the overburden and the gob.

If there is no support provided by the gob, the convergence of the seam in the panel for the homogeneous elastic model (s_h) can be determined as (Jaeger & Cook 1979):

$$s_h(x) = 4(1-\nu^2)\frac{\gamma H}{E}\sqrt{(L^2-x^2)} \qquad (21)$$

This equation states that the convergence of the seam in the panel is proportional to the depth (H) and to the distance from the edge of the panel ($L^2 - x^2$), and inversely proportional to the overburden modulus (E).

For the laminated overburden model, the formula for the convergence of the seam in the open panel (s_l) is very similar (Heasley 1998):

$$s_l(x) = \frac{\sqrt{12(1-\nu^2)}}{t}\frac{\gamma H}{E}(L^2-x^2) \qquad (22)$$

This equation states that the convergence of the seam in the panel is proportional to the depth (H) and to the square of the distance from the edge of the panel ($L^2 - x^2$), and inversely proportional to the overburden modulus (E) and lamination thickness (t). If ω is a constant as in equation 12; and therefore, the realistic lamination thickness is a function of the depth as in equation 13, then equation 22 can be written as:

$$s_l(x) = \frac{2\omega^2\gamma}{E}(L^2-x^2) \qquad (23)$$

In this equation, the convergence in the panel is now only proportional to the square of the distance from the edge of the panel ($L^2 - x^2$) and to the overburden constants ω and γ, and inversely proportional to the overburden modulus (E). Thus, once ω is considered to be a constant, the convergence across a panel in a given geology is also constant, regardless of the depth.

In general, gob material is considered to be strain-hardening such that the stiffness of the material increases with increasing strain. Basically, the granular/blocky gob material becomes stiffer as it is compacted and the void ratio decreases (Zipf 1992a, b). This exact response was documented by Pappas and Mark (1993) and incorporated into the MULSIM (Zipf 1992a, b) and the LAMODEL (Heasley 1998) programs using the following formula, where the gob stress (σ_g) is related to the gob strain (ε) by the equation:

$$\sigma_g = \left|\frac{E_i\sigma_u}{E_f - E_i}\right|\left|e^{\left(\frac{E_f - E_i}{n\sigma_u}\right)\varepsilon} - 1\right| \qquad (24)$$

where: E_i is the initial tangent modulus at zero stress,
E_f is the final tangent modulus at the ultimate stress (σ_u), and
n is the gob height factor (after Zipf 1992a b).

A schematic of the stress-strain curve for the material defined by equation 24 is given in Figure 6.

If the overburden displacement is considered to be linearly proportional to the depth (as with the homogeneous elastic overburden, equation 21, and the laminated overburden,equation 22) and the gob material is strain-hardening, then the gob should support an increasing percentage of load as the panel gets deeper. Therefore the percentage of the abutment load should decrease with depth (see curve 2 in Figure 5). If, on the other hand, the overburden displacement is constant with depth (as in equation 23 where the lamination thickness is proportional to the depth), then the change in the gob load will be

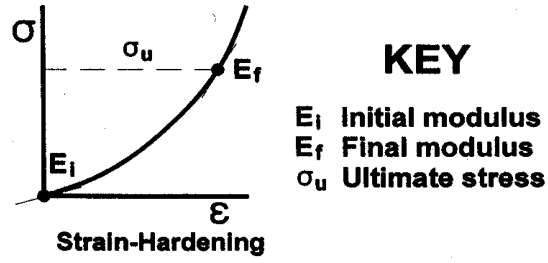

Figure 6. A schematic of the stress-strain relationship for the strain-hardening gob material.

proportional to the ratio between the gob modulus at the equilibrium stress and the modulus of the coal as in the third curve in Figure 5. For this third curve, the equilibrium gob modulus and the modulus of the coal are fairly equal; therefore the percentage of abutment load is fairly constant with changing depth. (For the LAMODEL plots in Figure 5, the input parameters were: a panel width of 200 m (L = 100), an extraction thickness (M) of 2 m, an elastic modulus of the rock mass (E) of 20 GPa, a Poisson's Ratio (ν) of the rock mass of 0.25, a constant lamination thickness (t) of 5.5 m or a constant ω of 7.0, an initial tangent modulus (E_i) of 0.69 MPa, a final tangent modulus (E_f) of 1.65 GPa, an ultimate stress (σ_u) of 27.6 MPa, and a gob height factor (n) of 1. For the various depth-to-width ratios, the depth was varied between 80 and 640 m.)

Within realistic limits for the equilibrium gob modulus, the third curve in Figure 5 could easily bend a little either down or up. However, it would have to be a very "soft" gob for the abutment load calculated using either the homogeneous elastic model or the laminated model to behave similarly to the behavior of the abutment load as calculated by the ALPS method in the first curve. This result derived from the analytical models, that the percentage of the overburden load carried on the abutments should be constant or even decrease with depth, suggests that the constant abutment angle used by the ALPS method over predicts the amount of the abutment load as the depth increases. A possible correction would be to decrease the ALPS's abutment as the overburden increases.

This actual trend was recently observed in Australian longwall panels (Colwell et al. 1999), where the apparent abutment angle was back calculated from field measurements and found to be much smaller than the ALPS default (21°) for the deeper panels. In fact, it was noted that: "the abutment angles calculated for the two deepest mines, ..., are the smallest of any in the database," 5.9° and 8.5°. A smaller abutment angle at depth would also help explain a conundrum with the "Analysis of Retreat Mining Pillar Stability" (ARMPS) method which also uses a constant abutment angle for calculating the pillar load (Mark & Chase 1997). In the ARMPS database, 70% of the case histories deeper than 300 m are successful with a Stability Factor less than 1.0.

CONCLUSIONS

Based on an analysis of the abutment stress implied by the empirically-derived ALPS method, the abutment stress derived from the homogeneous elastic model and the abutment stress derived from the laminated overburden model, a number of interesting results can be emphasized. First, using realistic parameters, the abutment load distribution used in the ALPS method is not very close to the load distributions determined from either the homogeneous elastic model or the laminated model. The abutment load distribution from the laminated model can be adjusted to fit the empirical abutment load distribution, but the parameter values needed to provide this degree of fit are unrealistic. Second, the laminated model analysis did suggest that the seam thickness, which is not included in the ALPS abutment load determination, may be an important factor to consider in determining the distribution of the abutment stress at the edge of an extraction panel. Finally, in comparing the response of the total magnitude of the abutment load to changes in depth as computed by the ALPS method, the homogeneous elastic model and the laminated model, it appears that the constant abutment angle used by the ALPS method probably over predicts the amount of the abutment load as the depth increases. This result suggests that some type of systematic decrease in the abutment angle with increasing depth may be more realistic.

REFERENCES

Barron, K. & Y. Pen 1992. Revised model for coal pillars. *Proceedings of the Workshop on Coal Pillar Mechanics and Design.* BuMines: IC 9315:144-157.

Bieniawski, Z.T 1968. In-situ strength and deformation characteristics of coal. *Eng. Geol.* 2(5):325-340.

Bieniawski, Z.T. 1983. New design approach for room-and-pillar coal mines in the USA. *5th ISRM Congress on Rock Mechanics*: E27-E36. Rotterdam: Balkema.

Colwell, M., R. Frith & C. Mark 1999. Analysis of longwall tailgate serviceability (ALTS): A chain pillar design methodology for australian conditions. *Proceedings of the Second International Workshop on Coal Pillar Mechanics and Design.* NIOSH: IC 9448:33-48.

Gaddy, F.L. 1956. A study of the ultimate compressive strength of coal. *Bulletin of the Virginia Polytechnic Institute Engineering experiment Station.* 112(August):1-27.

Hasenfus, G.J. & D.W.H. Su 1992. Comprehensive integrated approach for longwall development design. *Proceedings of the Workshop on Coal Pillar Mechanics and Design.* BuMines: IC 9315:225-237.

Heasley, K.A. 1998. Numerical modeling of coal mines with a laminated displacement discontinuity code. *Ph.D. Thesis.* Colorado: Colorado School of Mines.

Heasley, K.A. & T.M. Barton 1998. Subsidence prediction using a laminated, boundary-element

program. *Proceedings of the 3rd North American Rock Mechanics Symposium.* 2:381-390. Mexico Sociedad Mexicana del Mecánica de Rocas.

Holland, C.T. 1964. The strength of coal in mine pillars. *6th U.S. Symposium on Rock Mechanics:* 450-466. Missouri: University of Missouri.

Hustrulid, W. 1976. A review of coal pillar strength formula. *Rock Mechanics.* 8:115-145.

Jaeger, J.C. & N.G.W. Cook 1979. *Fundamentals of Rock Mechanics.* London: Chapman and Hall.

Mark, C. 1990. *Pillar design methods for longwall mining.* BuMines: IC 9247.

Mark, C. 1992. Analysis of longwall pillar stability (alps): an update. *Proceedings of the Workshop on Coal Pillar Mechanics and Design.* BuMines: IC 9315:238-249.

Mark, C. & F.E. Chase 1997. Analysis of retreat mining pillar stability (armps). *Proceedings: New Technology for Ground Control in Retreat Mining.* NIOSH: IC 9446:17-34.

Mark C. & A.T. Iannacchione 1992. Coal pillar mechanics: theoretical models and field measurements compared. *Proceedings of the Workshop on Coal Pillar Mechanics and Design,* BuMines: IC 9315:78-93.

Obert, L. & W.I. Duval 1967. *Rock mechanics and the design of structures in rock*: 531-545. New York: Wiley.

Pappas, D.M. & C. Mark 1993. *Behavior of Simulated Longwall Gob Material.* BuMines: RI 9458.

Park, D.W. 1992. Numerical modeling as a tool for mine design. *Proceedings of the Workshop on Coal Pillar Mechanics and Design.* BuMines: IC 9315:250-268.

Peng, S.S., & H.S. Chiang 1984. *Longwall mining.* New York: Wiley.

Salamon, M.D.G. 1992. Strength and stability of coal pillars. *Proceedings of the Workshop on Coal Pillar Mechanics and Design.* BuMines: IC 9315:94-121.

Salamon, M.D.G. 1989. Subsidence prediction using a laminated linear model. *Proceedings of the 30th U.S. Symposium of Rock Mechanics:* 503-510. Rotterdam: Balkema.

Salamon, M.D.G. & A.H. Munro 1967. A study of the strength of coal pillars. *J. S. Afr. Inst. Min. Metall.* 68:55-67.

Salamon, M.D.G. 1964. Elastic analysis of displacements and stresses induced by the mining of seam or reef deposits, part ii. *J. S. Afr. Inst. Min. Metall.* 64 (6):197-218.

Wagner, H. 1974. Determination of the complete load deformation characteristics of coal pillars. *3rd ISRM Congress on Rock Mechanics, Denver*: 1076-1081.

Wilson, A.H. 1973. An hypothesis concerning pillar stability. *Min. Eng. London.* 131(141) June:409-417.

Yang, G. 1992. Numerical approach to the prediction of subsidence due to longwall coal mining using a laminated model. *Ph.D. Thesis.* Colorado: Colorado School of Mines.

Zipf, R.K. 1992a. *Mulsim/nl application and practitioner's manual.* BuMines: IC 9322.

Zipf, R.K. 1992b. *Mulsim/nl theoretical and programmer's manual.* BuMines: IC 9321.